In vivo MRI of Injected Mesenchymal Stem Cells in Myocardial Infarction; Simultaneous Tracking and Functional Measurement

Young Jin Kim

Department of Medicine

The Graduate School, Yonsei University

In vivo MRI of Injected Mesenchymal Stem Cells in Myocardial Infarction; Simultaneous Tracking and Functional Measurement

Directed by Professor Kyu Ok Choe

The Doctoral Dissertation submitted to the
Department of Medicine,
the Graduate School of Yonsei University
in partial fulfillment of the requirements for the
degree of Doctor of Philosophy

Young Jin Kim

December 2006

This certifies that the Doctoral Dissertation
of Young Jin Kim is approved.

Thesis Supervisor : Kyu Ok Choe

Jin-Suck Suh

Yangsoo Jang

Jae Myun Lee

Yong-Min Huh

The Graduate School
Yonsei University

December 2006

ACKNOWLEDGEMENTS

I am grateful to prof. Kyu Ok Choe, thesis supervisor, for her consistent encouragement during the long and sometimes painful process of experiment and writing. I also acknowledge helpful comments of prof. Jin-Suck Suh, prof. Yong-Min Huh, prof. Yang Soo Jang, and prof. Jae Myun Lee.

I would like to express my great appreciation to my colleagues, Eun Jeong Choi, Il Kwon Kim, prof. Byoung Wook Choi, and my lovely husband, who inspired me to further efforts during the writing of this thesis.

TABLE OF CONTENTS

LIST OF FIGURES

LIST OF TABLES

ABSTRACT

In vivo MRI of Injected Mesenchymal Stem Cells in Myocardial Infarction: Simultaneous Tracking and Functional Measurement

Young Jin Kim

Department of Medicine

The Graduate School, Yonsei University

(Directed by Professor Kyu Ok Choe)

Purpose: The purpose of this study was to determine if magnetically labeled mesenchymal stem cells (MSCs) could be imaged and whether cardiac function could be simultaneously evaluated *in vivo* in a rat model of myocardial infarction using MRI.

Methods and Materials: Myocardial infarction was induced in rat myocardium (male, SD rat) by cryoinjury. Human MSCs were labeled with superparamagnetic iron oxide particles (ferumoxides, Feridex®) and injected into the infarcted myocardium three weeks after the injury. In the control group, cell-free media was injected. *In vivo* MRI was serially performed before and after cell injection during three months using a 1.5-T clinical scanner with 47-mm microcoil. For *in vivo* cell tracking, gradient echo sequence with ECG gating was used. For evaluation of cardiac function, global and regional left ventricular ejection fraction (LVEF) was measured using cine MRI.

Results: Feridex-labeled MSCs were visualized as a signal void on *in vivo* MRI until 10 weeks after injection. On serial follow-up MRI, the ejection fraction was significantly higher in the MSC injection group (EF=54.5± 4.5%) than in the control group (EF=34.0± 2.2%).

Conclusion: These results support the ability of MRI to track injected cells in vivo as well as to evaluate long term therapeutic potential of mesenchymal stem cells for

myocardial infarction.

Key words: magnetic resonance imaging, iron oxide, myocardial infarction, mesenchymal stem cell, rats

In vivo MRI of Injected Mesenchymal Stem Cells in Myocardial Infarction; Simultaneous Tracking and Functional Measurement

Young-Jin Kim

Department of Medicine
The Graduate School, Yonsei University

(Directed by Professor Kyu Ok Choe)

Ⅰ. INTRODUCTION

Advances in cell therapy (e.g. stem cell transplantation) have produced increasing interest in noninvasive *in vivo* imaging of transplanted cells. Imaging of *in vivo* cellular and molecular events can be achieved with various imaging technologies including nuclear imaging, optical imaging, and magnetic resonance imaging (MRI)[1-5]. Nuclear imaging has excellent sensitivity; however, with this method, spatial resolution is very low and radionuclides must be used[1]. Optical imaging is highly sensitive, but because light dose not penetrate deep into tissue, imaging is limited to skin or superficial tissue and thus, *in vivo* spatial resolution is low[2-4]. Though the sensitivity of iron-oxide probes used in MRI is lower than that of nuclear and optical imaging, MRI has many advantages, including its noninvasive nature, its use of non-radioactive substrates, its multi-dimensional tomographic capabilities, and its excellent *in vivo* spatial resolution[5].

The development of cellular therapies will require new techniques such as the labeling of cells with magnetic nanoparticles, like superparamagnetic iron oxides (SPIO), and *in vivo* cell tracking using MRI, which is useful in determining the fate of

transplanted stem cells[6-8].

Recently, functional improvement was reported after injection of stem cells, both in animal models of myocardial infarction and in the patients with myocardial infarction[9-16]. In previous reports of small animal experiments, cardiac function was evaluated using invasive pressure measurement,[9, 10, 17] and transplanted cells were identified only in extracted tissue specimen[9-12, 18, 19]. *In vivo* tracking of transplanted cells was not achieved in previous human clinical studies[13-16]. For clinical application of stem cell therapy in patients with myocardial infarction, *in vivo* functional evaluation and cell tracking is mandatory, unlike in animal experimentation.

The purpose of this study is to determine if magnetically labeled mesenchymal stem cells could be imaged *in vivo* in a rat model of myocardial infarction, and whether cardiac function could be simultaneously evaluated using MRI.

II. MATERIALS AND METHODS

1. Cell preparation and labeling

Mesenchymal stem cells (MSCs) were isolated from human bone marrow and grown at 37°C in a 5% CO_2 incubator. Dulbeco's Modified Eagle Medium (DMEM, Gibco, Carlsbad, CA, USA) including 10 percent of fetal bovine serum (FBS, Gibco, Carlsbad, CA, USA) and penicillin-streptomycin (Invitrogen, Carlsbad, CA, USA) was used as a standard culture medium.

To label the MSCs, we used ferumoxides (Feridex, Berlex Laboratories, Wayne, NJ, USA) combined with protamine sulfate (American Pharmaceuticals Partner, Schaumburg, IL, USA) as a transfection agent[20, 21]. Feridex (50 μg/ml) and protamine sulfate (9 μg/ml) were added to the standard culture medium and then mixed for 10 minutes with intermittent hand shakings. After incubation with the medium containing Feridex-protamine sulfate complex for 2 hours, an equal volume of the standard culture medium was added to the adherent cell culture (final concentration; Feridex=25 μg/ml, protamine sulfate=4.5 μg/ml) and then incubated overnight. After overnight incubation, the medium was discarded and the cells were washed twice with heparin containing phosphate buffered saline, treated with trypsin, collected, rewashed, and counted to adjust the cell concentration for injection.

The degree of intracellular labeling was checked by Prussian blue stain. Labeled 10^5cells were transferred to a cytospin slide. Cells were fixed with 95% alcohol, washed, incubated for 20 minutes with 10% potassium ferrocyanide (Perl's reagent for Prussian blue staining) and 3.7% hydrochloric acid, washed again, and counterstained with nuclear fast red.

Cells were considered Prussian blue positive if intracytoplasmic blue inclusions were detected. Labeling efficiency was determined by manual counting of Prussian blue-stained and unstained cells using a hemocytometer at 100x magnification.

2. *In vitro* toxicity assays

Viability of labeled cells (the MSCs that were incubated with 25μg/ml Feridex and 4.5μg/ml protamine sulfate) and unlabeled cells was assessed by the MTT (3-(4,5-dimethylthiazol-2-yl)-2,5-diphenyl tetrasodium bromide, Roche Diagnostics GmbH, Penzberg, Germany) assay. The absorbance of formazen product, which indicates levels of mitochondrial activity, was measured at the 4th day of culture.

3. Determination of magnetic sensitivity of Feridex-labeled MSCs

Magnetic sensitivity of Feridex-labeled MSCs, as measured by the number of the cells, was tested using T2 mapping MRI. For MRI, the number of labeled cells ranged from 10^4 to 10^7cells, and these cells were put in PCR tubes and a cell suspension was made with 0.5% agarose gel.

4. Rat myocardial infarction model and MSC injection

We studied twenty male Sprague-Dawley rats (SLC, Tokyo, Japan), weighing 150−200g. After anesthesia with an intraperitoneal injection of ketamine and xylazine, the rats were intubated and placed on a mechanical ventilator (Model 683, Harvard Apparatus, South Natick, MA, USA). Under mechanical ventilation, the heart was exposed following left lateral thoracotomy, and cryoinjury was induced with a cooled (-190°C with liquid nitrogen) metal rod (8mm in diameter, stainless steel), as previously described[18, 22, 23]. The cooled metal rod was applied to the left ventricle (LV) free wall for 25 seconds four times. The damaged area was grossly identified as a firm white disk-shaped region at the anterior and lateral wall of mid to apical LV. After the injury, the chest was closed with sutures.

Three weeks later, mid sternotomy was done under deep anesthesia and mechanical ventilation and then Feridex-labeled MSCs ($1.0x10^7$ in number, 100 μl in volume) were injected intramyocardially at the border of the infarction (at the area of

subepicardial infarction) with a 31-gauge needle (n=15). As a control group (sham operation), five rats were injected with an equal volume of cell-free media.

5. MRI for *in vivo* tracking and evaluation of cardiac function

MRI was obtained with a 1.5-T clinical MRI instrument with a 47-mm microcoil and vectorcardiogram (Intera Achieva, Philips Medical Systems, Best, Netherlands).

Baseline MRI was performed within two weeks after the cryoinjury to evaluate baseline cardiac function. Immediate *in vivo* MRI was taken three days after MSC injection to identify the injection site and determine engraftment. Long-term follow-up MRI was taken during 10 weeks after MSC injection or sham operation.

For evaluation of normal cardiac function in rat, cine MRI of normal rats without surgery (n=5) was performed.

6. MR sequence and analysis

A. *In vitro* MR protocol

For determination of magnetic sensitivity of Feridex-labeled MSCs, T2 mapping sequence was performed: TR=2000ms, TE=20~160ms, number of averages=2, matrix=256 x 256, field of view=60mm, slice thickness=2mm. T2 value of the suspension of labeled cells was measured by region of interest (ROI) analysis of T2 mapping image using the software available on the MR unit.

B. *In vivo* MR protocol and analysis

For *in vivo* cardiac MRI, the rats were anesthetized by the same procedure used for surgery, and electrodes were placed on the feet for electrocardiography (ECG) triggering. *In vivo* MRI to visualize Feridex-labeled MSCs was conducted by applying ECG triggered gradient echo sequence with the following parameters: T1-turbo field echo sequence, shortest TR and TE, flip angle=15°, matrix=128 x 256, slice thickness=2mm, number of signal averages=6, field of view=100mm, inversion time=540ms.

For evaluation of cardiac function, we acquired cine MRI with 7 to 8 contiguous

short-axis slices to cover the entire heart from base to apex. Detailed parameters were as follows: fast field echo sequence, shortest TR and TE, flip angle=50°, matrix=256x128, slice thickness=2mm/ no gap, number of signal averages=2, field of view=120mm, frames per cardiac cycle=14~20.

Global and regional left ventricular ejection fraction (LVEF) and end-diastolic dimension (EDD) was measured. Global LVEF was calculated by (end-diastolic volume − end-systolic volume)/end-diastolic volume x 100 (%) by depicting endocardial borders of end-diastolic and end-systolic phase images with a dedicated software package (ViewForum, Philips Medical Systems, Best, Netherlands). We defined regional EF as an EF of each short axis slice. Regional LVEF was obtained from volumetric data of each slice of short axis cine images and the first (apical) and the last (basal) slices were excluded from the analysis. We measured regional EF as a regional function parameter because commonly used systolic wall thickening could not be measured due to low spatial resolution of the 1.5-T clinical scanner.

EDD was measured at the end-diastolic phase image of cine MRI taken at the mid LV level.

7. Histological Analysis

One, two, and six weeks after MSC injection, the rats were sacrificed. Whole hearts were retrieved and fixed in 4% paraformaldehyde. The specimens were cut into 4 μm sections in the short-axis plane and stained with hematoxylin and eosin (H&E) and Masson’s trichrome method. Prussian blue stain was performed to detect Feridex-labeled MSCs. For identification of the origin of the Prussian blue positive cells, mouse anti-human nuclei monoclonal antibody (HuNu, Chemicon, Temecula, CA, USA) stain was used.

III. RESULTS

1. Cell labeling

Feridex-labeled MSCs showed abundant intracytoplasmic blue inclusions following Prussian blue staining (Fig. 1). Using the Feridex-protamine sulfate complex for cell labeling, labeling efficiency was 100%.

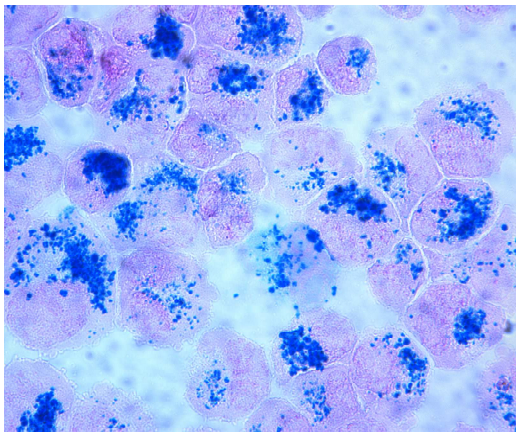

Figure 1. Prussian blue-stained Feridex-labeled MSCs (magnification of 100x).

2. *In vitro* toxicity assays

The MTT-based toxicity and proliferation assay demonstrated no statistically significant decrease in labeled MSC viability compared with that of the unlabeled MSCs. There was no significant difference in optical density which would have indicated differences in mitochondrial enzymatic activity between labeled (0.816 ± 0.04) and unlabeled cells (0.803 ± 0.02) (Table 1).

OD	Sample 1	Sample 2	Sample 3	**Average**
Labeled MSC	0.789	0.802	0.856	0.816 ± 0.04
Unlabeled MSC	0.778	0.811	0.821	0.803 ± 0.02

Table 1. Viability of labeled and unlabeled MSCs with MTT assay.

There are no significant differences in viability values between labeled and unlabeled cells (p=0.4345). OD indicates optical density.

3. Magnetic sensitivity of Feridex-labeled MSCs

Magnetic sensitivity of Feridex-labeled MSCs, as measured by the number of the cells, is shown in Figure 2. T2 mapping MRI confirmed that the T2 value decreased as the number of the cells increased. Susceptibility artifact occurred in experiments where 10^7 cells were used. According to these results, 1.0 x 10^7 cells were determined as the number of cells for intramyocardial injection, considering that many cells are required for *in vivo* detection during long-term follow up and that cells may leak during intramyocardial injection.

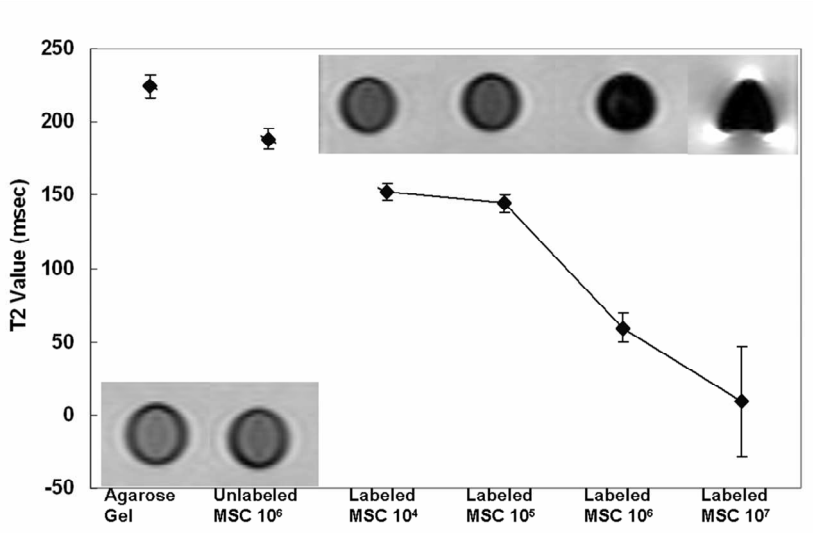

Figure 2. T2 values of suspensions of Feridex labeled MSCs according to the cell number.

4. Myocardial infarction model by cryoinjury

After cryoinjury, the damaged area was grossly identified as a firm white disk-shaped lesion positioned at the anterior and lateral wall. The lesion extended from the upper mid to the apical level of the LV (Fig 3A). Using histological sections (Fig. 3B and 3C), wall thinning was demonstrated at the anterior wall and lateral wall of the LV at the mid to apical level, and the infarcted myocardium was replaced with fibrosis (blue area on Fig. 3C). The center of the injury was transmural infarction and

the periphery was subepicardial infarction.

MSCs were injected in the nine o'clock direction between apical LV and mid LV, which on gross was assumed as the border of myocardial infarction. Pathologically this lesion was confirmed as subepicardial infarction. (black circles on Fig. 3).

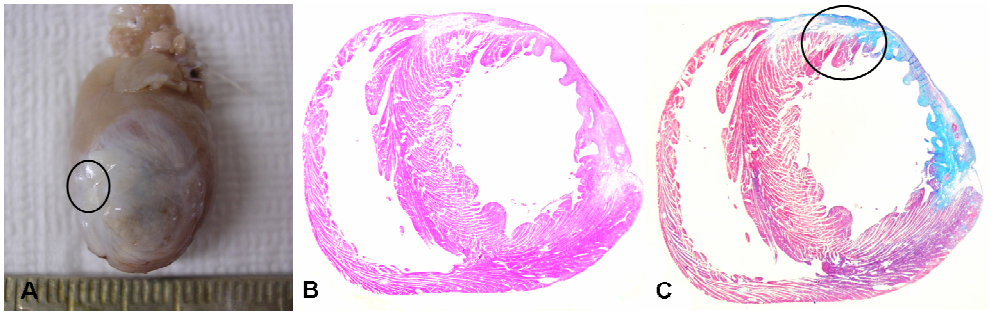

Figure 3. Gross specimen (A) and histological sections (B; H & E stain, C; Masson's trichrome stain) of heart 3 weeks after cyroinjury. Black circles demonstrate the MSC injection site.

5. *In vivo* MR tracking of MSCs

In vivo MRI of the rat hearts damaged by cryoinjury showed thinning of the anterior and lateral wall of the LV (Fig. 4), as well as akinesia. A round signal-void lesion corresponding to the injection site was observed in the *in vivo* MRI of all 15 rats injected with Feridex-labeled cells (Fig. 4A). In the control group injected with cell-free media, signal-void lesions were not detected at the injection sites (Fig. 4B).

Serial MRI studies demonstrated persistent signal void at the injection site until 10 weeks, during which time this signal void effect remained with a slight narrowing and elongation (Fig. 5). There was no visible signal-void lesion in the remote myocardium from the injection site.

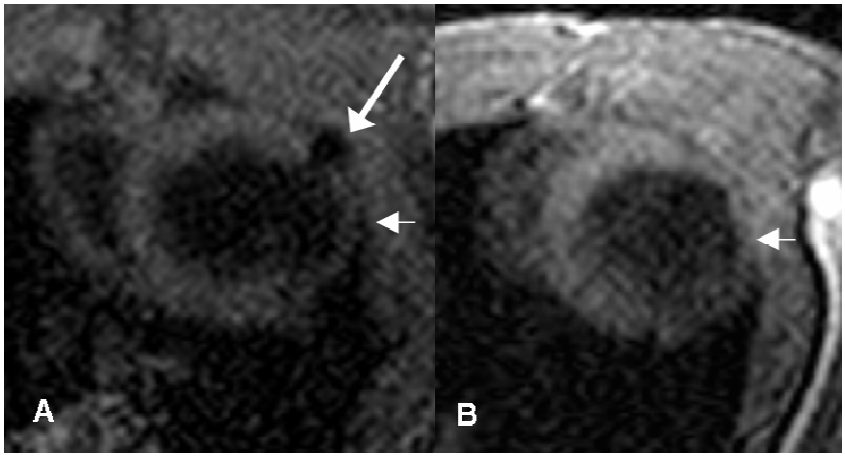

Figure 4. In vivo MRI three days after MSC injection and sham operation.

Short axis T1 weighted images of the rat with Feridex-labeled MSC injection (A) shows the distinct signal dropout (thick arrow) that is not observed in the control rat (B). Left ventricular wall thinning (thin arrows) is noted at the cryoinjury site.

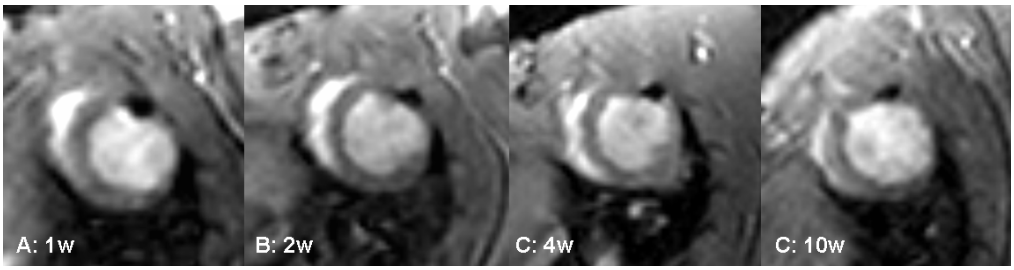

Figure 5. In vivo serial MRI.

Serial short-axis views imaged at 1, 2, 4, and 10 weeks show a persistent signal void after injection of Feridex-labeled MSCs.

6. Cardiac function by MRI

In normal rats without cryoinjury (n=5), global left ventricular ejection fraction (LVEF) measured 72.9±1.7%. Baseline global LVEF after cryoinjury measured 44.0±4.8%. There was no significant difference in the baseline global LVEF and EDD between the MSC injection group (EF; 44.9±5.1%, EDD; 8.25±0.75 mm) and the control group (EF; 42.9±4.7%, EDD; 8.31±0.26 mm).

On serial follow-up MRI, global LVEF was significantly higher in the MSC

injection group (EF=54.5± 4.5%) than in the control group (EF=34.0± 2.2%) ($p<0.0001$) (Fig. 6A). There was no statistically significant difference of EDD between the two groups although EDD was slightly larger in the control group than in the MSC injection group (Fig.6B).

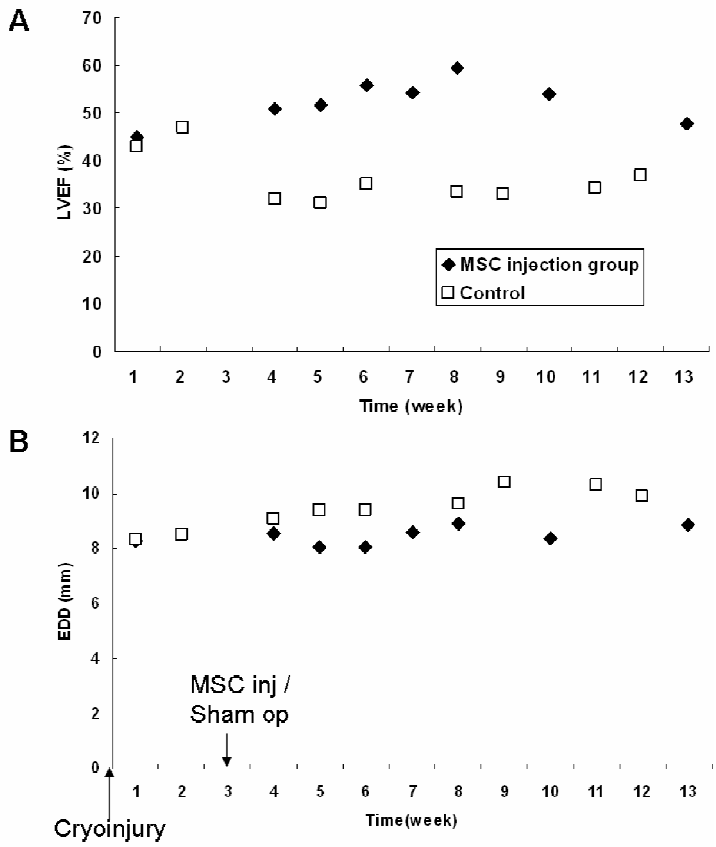

Figure 6. Changes in global systolic function and left ventricular dimension after MSC injection.
LVEF= global left ventricular ejection fraction, EDD=end-diastolic dimension.

Changes in regional ejection fraction (EF) were demonstrated in Figure 7. In our myocardial infarction model of cryoinjury, baseline regional EF was decreased at the apical and mid parts. The MSC injection site corresponded to the second or third short axis slice in Figure 7. In the MSC injection group, regional EF of mid and apical parts of LV was significantly improved after 2 and 5 weeks following MSC injection (Fig.

7A). However, regional EF of mid and apical parts was more greatly deteriorated in the control group (Fig. 7B).

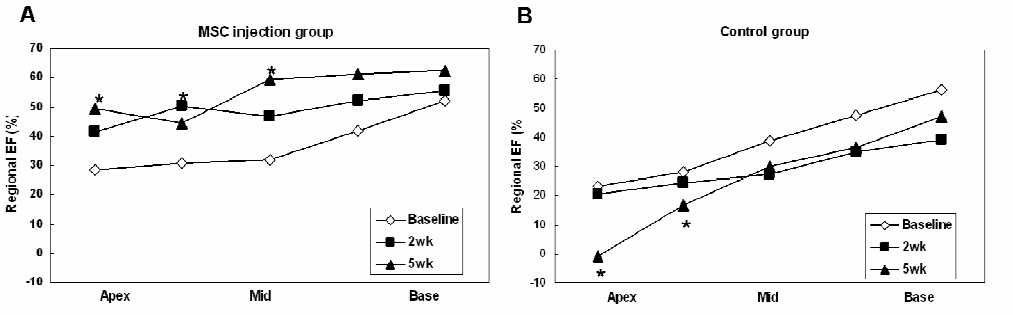

Figure 7. Changes in regional left ventricular function after MSC injection.

* indicates statistically significant ($p<0.05$) difference from baseline regional EF. EF=ejection fraction

7. Histological Analysis.

In extracted heart from the rats injected with Feridex-labeled MSCs, Prussian blue stain showed dense intracellular iron labeled cells. After 1 week of injection, Prussian blue positive cells were detected in sections corresponding to the signal-void lesions seen on MRI (Fig. 8A and 8B). Apart from the injection site, Prussian blue positive cells were elongated and the axis of elongation of each cell extended in same direction (Fig. 8C), suggesting a migratory cell population. However, this portion was not demonstrated as signal void lesion on MRI.

Prussian blue positive cells were still detected on the specimens extracted at 2 and 6 weeks after MSC injection.

Because the Prussian blue positive cells could potentially represent phagocytic macrophages that contain native iron or that have ingested Feridex from lysed MSCs, immunohistochemical staining was performed with anti-human nuclei antibody. Immunohistochemical stain confirmed that the Prussian blue positive cells were injected Feridex-labeled MSCs and Feridex remained within the originally labeled cells (Fig. 9).

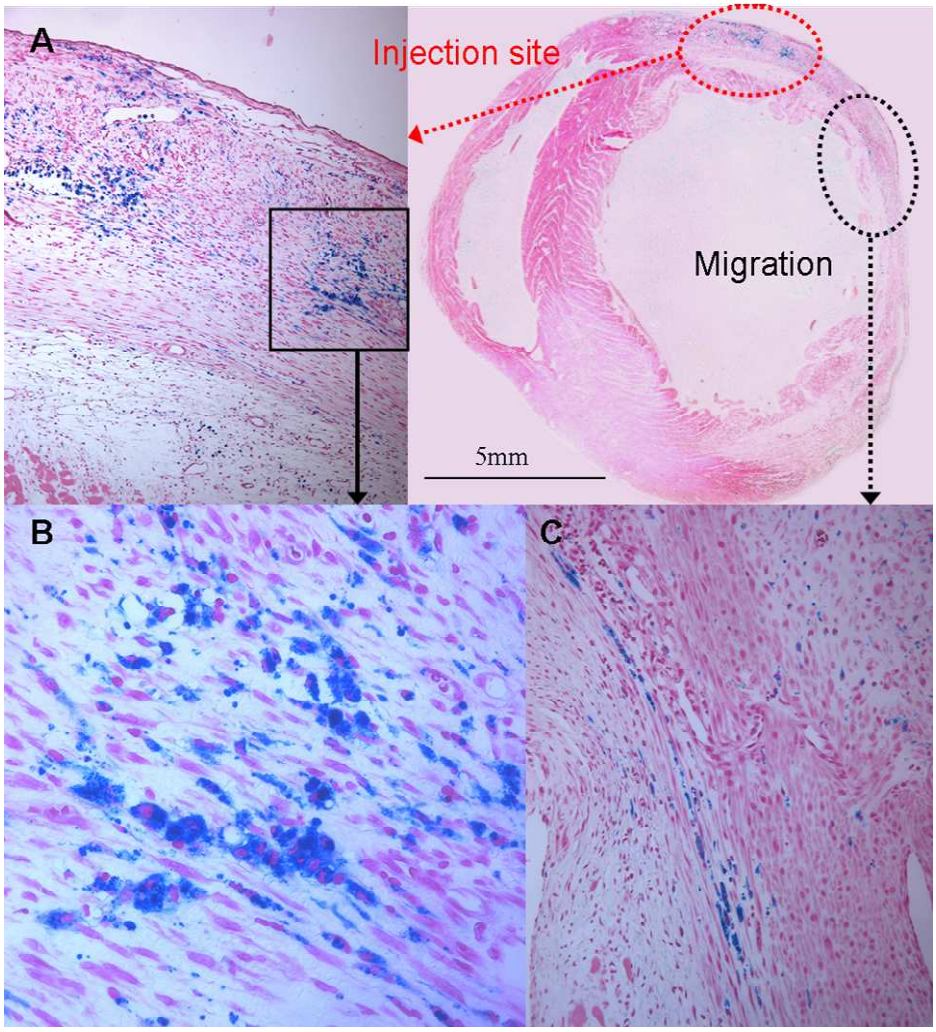

Figure 8. Histologic section with Prussian blue stain at 1 week after Feridex-labeled MSC injection. (A) In the MSC injection site, multiple blue colored cells are shown (red circle, x100). (B)Multiple cells with blue inclusion are noted in the high power field (x400). (C) Blue colored cells that were elongated and were positioned in same direction were found away from the injection site (black circle, x200).

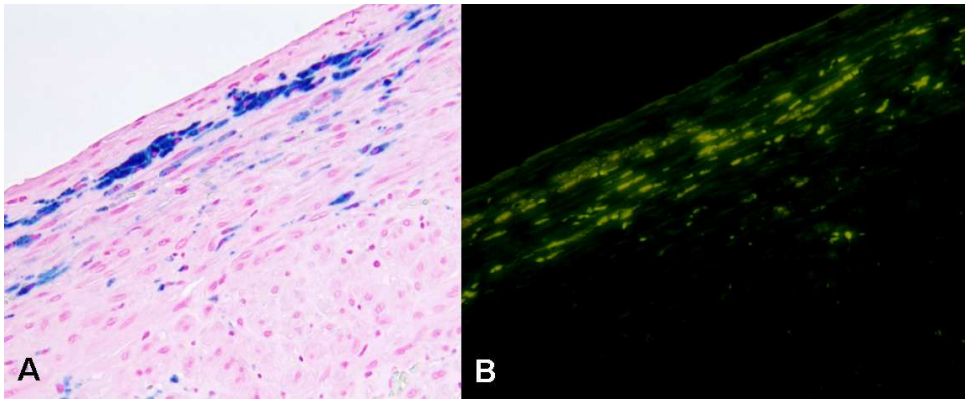

Figure 9. Validation of the origin of iron containing cells with immunohistochemistry. Prussian blue stain (A) shows multiple iron containing blue colored cells at the infarcted site (x200). Immunohistochemical stain with anti-human nuclei antibody stain (B) validates the origin of the Prussian blue positive cells are the injected MSCs.

IV. DISCUSSION

The ability of track movements of transplanted stem cells is of increasing importance in cell therapy (e.g. stem cell transplantation). Of particular interest is the use of MRI to monitor the *in vivo* behavior of stem cells with MR contrast agents such as superparamagnetic iron oxide (SPIO) nanoparticles.

To determine the fate of transplanted cells, cells are traditionally labeled *ex vivo* using a vital dye, a thymidine analog, or a transfected gene, for later visualization using immunohistochemical procedures following tissue removal. Labeling cells with MR contrast agents, however, provides a means of identifying and tracking the migration of labeled cells following infusion or transplantation *in vivo*.

Various approaches have been developed to label cells with MR contrast agents *ex vivo* prior to transplantation[8, 20, 21, 24-29]. MR contrast agents can be incorporated into nonphagocytic cells through receptor-mediated endocytosis, macropinocytosis, or mechanical means such as electroporation[30]. Macropinocytosis is an active process starting as a membrane extension from the plasma membrane, eventually forming micropinosomes, and is the presumed mechanism for which arginine-containing protein transduction domains including polyarginine, Tat proteins, peptides, polycationic transfection agents and liposomes are incorporated into the cell[25, 31, 32].

In the present study, two FDA-approved commercially available agents, ferumoxides (Feridex) and protamine sulfates, were successfully used to label cells. Ferumoxides are suspensions consisting of dextran-coated SPIO nanoparticles with high negative charges. When used alone, ferumoxides do not efficiently label nonphagocytic cells without modification of nanoparticle surface charges, therefore, polycationic transfection agents should be used for efficient intracellular labeling[8, 25].

Poly-L-lysine (PLL) has been widely used as a polycationic transfection agent, however, it is not FDA approved for human use and the incubation time of PLL with ferumoxides affects the growth and size of the ferumoxides-PLL complex, ultimately forming macroscopically visible particles that usually do not get incorporated into the

endosomes of cells[21]. Hence, there is a possibility of overestimation of the total amount of iron per cell due to adherence of complexes to cell membranes without incorporation into the endosomes. In the current study, protamine sulfate was used as a transfection agent. Protamine sulfate is a naturally occurring peptide containing approximately 60−70% of arginine residues. It is used clinically worldwide as an antidote to heparin-induced anticoagulation and is well-tolerated by cells, and thus has a high therapeutic window[33]. Arbab AS *et al.* recently reported that magnetic labeling of cells with ferumoxides-protamine sulfate complexes is comparable or superior to other methods, and addition of heparin to cell washes after labeling can completely dissolve surface-bound particles of ferumoxides-protamine sulfate complexes through competition, therefore, very clean labeling is possible with minimum extracellular iron complex formation[20, 21]. In our study, we determined that cell labeling with this ferumoxides-protamine sulfate method was very efficient and clean without residual extracellular iron complexes.

In the most of the previous small animal myocardial infarction studies about stem cell transplantation, either extracted pathologic specimens or *ex vivo* MRI has enabled identification of transplanted cells into the myocardium[9-12, 18, 19, 34], and *in vivo* MR tracking was only tried using a high-Tesla scanner[35]. In those studies, functional evaluation after stem cell transplantation was done using pressure measurements through a Millar catheter or with the Langendorf method, which is not commonly used in the clinical setting. There were several reports on *in vivo* identification of magnetically labeled cells in large animals such as swine or canine models using MRI [36-40]. Those studies demonstrated that *in vivo* MR tracking of magnetically labeled cells is feasible with a clinical MR scanner, however, functional evaluation using MRI was not done. A preliminary report by Rickers C *et al.* recently demonstrated the potential of MRI for image-guided interventions, combined with detailed evaluation of function, perfusion, and viability[41]. Therefore, in the current study, we aimed to identify transplanted cells *in vivo* and simultaneously measure cardiac function using

a clinical MR scanner in a rat model of myocardial infarction.

In the present study, cryoinjury was used as a model of experimental myocardial infarction to make constant infarct size, location, and cardiac dysfunction. Coronary ligation is the standard technique[42], but is limited in rats because it produces variable and unpredictable areas of necrosis. However, cryoinjury has the advantage of reproducibility because it can cause the same degree and location of infarction. If compared with ischemic infarcts, cryoinjury causes subepicardial infarction with no transition zone to noninfarcted myocardium, while it reproduces the cellular patterns of coagulation necrosis, microvascular reperfusion, hemorrhage, inflammation, and scarring observed in myocardial infarction[22, 43, 44].

We were able to detect the intramyocardial injection sites of MSCs in the rat heart by *in vivo* MRI. On MRI immediately after Feridex-labeled MSCs were injected, injection sites appeared as round signal-void lesions. The SPIO nonoparticles shorten the T1, T2 and T2* relaxation times of water or tissue and have a high T2 relaxivity/T1 relaxivity ratio and significant capacity to reduce MRI signal, which can be emphasized by using spin echo sequences with longer echo time and gradient echo sequences[45]. Therefore, intracellular SPIO of transplanted cells could be readily detected as a signal void (dark lesion) by conventional cardiac MR.

The signal-void lesions were decreased in size and elongated in shape but still detected after 10 weeks. Persistence of signal-void lesions might not directly indicate viability of the injected MSCs because iron oxides can remain at the injection sites even if cells are dead. However, recent studies found that SPIO released from dead grafted cells seems to exit the myocardium through a specific pathway in a short period of time[36, 40]. Therefore, the void signals seen in follow-up MRI could be produced by the intracytoplasmic SPIO in the survived cells, which gives us hints that the surviving cells exist in the myocardium, and any changes of the signals will also give us useful information about the migration of the transplanted cells. We think the change of contour into the elongated shape represents migration of Feridex-labeled MSCs, because we found migrated MSCs apart from the injection site in the

histologic specimens; however, MRI did not demonstrate distant migration and only showed a mild change of contour into an elongated shape, probably due to low spatial resolution and low sensitivity of MRI in detecting SPIO-labeled cells. Low sensitivity of MRI was also reported by Kraitchman DL *et al*[46]. In that study, intravenously injected MSCs that were co-labeled with a radiotracer and MR contrast agent were visible in SPECT/CT scanner, but MRI was unable to demonstrate MSCs because of lower sensitivity. To overcome this limitation, more sensitive MR contrast agents and more efficient labeling techniques should be further investigated.

In vivo detection of magnetically labeled cells by MRI has another limitation. The contrast in the image relies on a susceptibility artifact, which implies that it is difficult to quantify the number of labeled cells in target tissues. Development of a positive-contrast technique, or continuously evolving MR hardware and pulse sequences, could solve this problem in the future.

On the other hand, MRI has the powerful advantage of being a tool to evaluate function. With it, we were able to evaluate cardiac function simultaneously. In our results, global LVEF of the MSC injection group was improved after MSC injection, while global LVEF of the control group markedly worsened after sham operation. When we analyzed regional EF in each short axis slice, dysfunction of apical and mid LV was gradually aggravated in the sham operation group. Therefore, worsening of global LV systolic function after sham operation could be explained due to progression of harmful LV remodeling, which is the natural course of cyroinjury[22], whereas MSC injection is supposed to improve regional function and to prevent harmful LV remodeling, and eventually improve global ejection fraction in the MSC injection group. Our results regarding the favorable effect of MSC injection on regional LV function correspond with the results of two recent human clinical trials[47, 48] and a large animal study[49]. EDD was not significantly different between the two groups, which may be due to a small number of rats, low resolution of the images and inaccurate short axis localization during MR scan.

The current study did not examine the differentiation of the injected MSCs because

the primary goal of this study was to determine if magnetically labeled MSCs could be imaged *in vivo* in a rat model of myocardial infarction, and whether cardiac function could be simultaneously evaluated using MRI. According to previous studies on transplantation of MSCs into the ischemic myocardium, injected MSCs differentiate into endothelial cells and cardiomyocytes and improve cardiac structure and function by enhancing cytoprotection, angiogenesis and myogenesis[11, 50-53].

In summary, our results demonstrate that MSCs labeled with Feridex can be tracked *in vivo* in the myocardium of rats after cryoinjury, and that the ejection fraction can be serially measured using MRI. The ability of MRI to track cells noninvasively while simultaneously measuring cardiac function should offer significant clinical advantages in cardiac stem cell therapy.

V. CONCLUSION

MRI allows tracking of injected cells *in vivo* while simultaneously evaluating cardiac function in the rat heart cryoinjury model. In the clinical trials involving cell transplantation to treat cardiac disease, MRI could be a potentially valuable tool for *in vivo* tracking and monitoring of therapeutic outcome.

REFERENCES

1. Ray P, Wu AM, Gambhir SS. Optical bioluminescence and positron emission tomography imaging of a novel fusion reporter gene in tumor xenografts of living mice. Cancer Res 2003; 63:1160-1165.
2. Weissleder R, Ntziachristos V. Shedding light onto live molecular targets. Nat Med 2003; 9:123-128.
3. Wu JC, Chen IY, Sundaresan G, Min JJ, De A, Qiao JH, et al. Molecular imaging of cardiac cell transplantation in living animals using optical bioluminescence and positron emission tomography. Circulation 2003; 108:1302-1305.
4. Ntziachristos V, Bremer C, Weissleder R. Fluorescence imaging with near-infrared light: new technological advances that enable in vivo molecular imaging. Eur Radiol 2003; 13:195-208.
5. Gillies RJ. In vivo molecular imaging. J Cell Biochem Suppl 2002; 39:231-238.
6. Bulte JW, Douglas T, Witwer B, Zhang SC, Strable E, Lewis BK, et al. Magnetodendrimers allow endosomal magnetic labeling and in vivo tracking of stem cells. Nat Biotechnol 2001; 19:1141-1147.
7. Lewin M, Carlesso N, Tung CH, Tang XW, Cory D, Scadden DT, et al. Tat peptide-derivatized magnetic nanoparticles allow in vivo tracking and recovery of progenitor cells. Nat Biotechnol 2000; 18:410-414.
8. Frank JA, Miller BR, Arbab AS, Zywicke HA, Jordan EK, Lewis BK, et al. Clinically applicable labeling of mammalian and stem cells by combining superparamagnetic iron oxides and transfection agents. Radiology 2003; 228:480-487.
9. Min JY, Yang Y, Sullivan MF, Ke Q, Converso KL, Chen Y, et al. Long-term improvement of cardiac function in rats after infarction by transplantation of embryonic stem cells. J Thorac Cardiovasc Surg 2003; 125:361-369.

10. Min JY, Yang Y, Converso KL, Liu L, Huang Q, Morgan JP, et al. Transplantation of embryonic stem cells improves cardiac function in postinfarcted rats. J Appl Physiol 2002; 92:288-296.
11. Silva GV, Litovsky S, Assad JA, Sousa AL, Martin BJ, Vela D, et al. Mesenchymal stem cells differentiate into an endothelial phenotype, enhance vascular density, and improve heart function in a canine chronic ischemia model. Circulation 2005; 111:150-156.
12. Fernandez-Aviles F, San Roman JA, Garcia-Frade J, Fernandez ME, Penarrubia MJ, de la Fuente L, et al. Experimental and clinical regenerative capability of human bone marrow cells after myocardial infarction. Circ Res 2004; 95:742-748.
13. Wollert KC, Meyer GP, Lotz J, Ringes-Lichtenberg S, Lippolt P, Breidenbach C, et al. Intracoronary autologous bone-marrow cell transfer after myocardial infarction: the BOOST randomised controlled clinical trial. Lancet 2004; 364:141-148.
14. Kang HJ, Kim HS, Zhang SY, Park KW, Cho HJ, Koo BK, et al. Effects of intracoronary infusion of peripheral blood stem-cells mobilised with granulocyte-colony stimulating factor on left ventricular systolic function and restenosis after coronary stenting in myocardial infarction: the MAGIC cell randomised clinical trial. Lancet 2004; 363:751-756.
15. Assmus B, Schachinger V, Teupe C, Britten M, Lehmann R, Dobert N, et al. Transplantation of Progenitor Cells and Regeneration Enhancement in Acute Myocardial Infarction (TOPCARE-AMI). Circulation 2002; 106:3009-3017.
16. Strauer BE, Brehm M, Zeus T, Kostering M, Hernandez A, Sorg RV, et al. Repair of infarcted myocardium by autologous intracoronary mononuclear bone marrow cell transplantation in humans. Circulation 2002; 106:1913-1918.
17. Nakamura Y, Yasuda T, Weisel RD, Li RK. Enhanced cell transplantation: preventing apoptosis increases cell survival and ventricular function. Am J

Physiol Heart Circ Physiol 2006; 291:H939-947.

18. Ciulla MM, Lazzari L, Pacchiana R, Esposito A, Bosari S, Ferrero S, et al. Homing of peripherally injected bone marrow cells in rat after experimental myocardial injury. Haematologica 2003; 88:614-621.
19. Jackson KA, Majka SM, Wang H, Pocius J, Hartley CJ, Majesky MW, et al. Regeneration of ischemic cardiac muscle and vascular endothelium by adult stem cells. J Clin Invest 2001; 107:1395-1402.
20. Arbab AS, Yocum GT, Kalish H, Jordan EK, Anderson SA, Khakoo AY, et al. Efficient magnetic cell labeling with protamine sulfate complexed to ferumoxides for cellular MRI. Blood 2004; 104:1217-1223.
21. Arbab AS, Yocum GT, Wilson LB, Parwana A, Jordan EK, Kalish H, et al. Comparison of transfection agents in forming complexes with ferumoxides, cell labeling efficiency, and cellular viability. Mol Imaging 2004; 3:24-32.
22. Ciulla MM, Paliotti R, Ferrero S, Braidotti P, Esposito A, Gianelli U, et al. Left ventricular remodeling after experimental myocardial cryoinjury in rats. J Surg Res 2004; 116:91-97.
23. Ryu JH, Kim IK, Cho SW, Cho MC, Hwang KK, Piao H, et al. Implantation of bone marrow mononuclear cells using injectable fibrin matrix enhances neovascularization in infarcted myocardium. Biomaterials 2005; 26:319-326.
24. Frank JA, Zywicke H, Jordan EK, Mitchell J, Lewis BK, Miller B, et al. Magnetic intracellular labeling of mammalian cells by combining (FDA-approved) superparamagnetic iron oxide MR contrast agents and commonly used transfection agents. Acad Radiol 2002; 9 Suppl 2:S484-487.
25. Arbab AS, Bashaw LA, Miller BR, Jordan EK, Bulte JW, Frank JA. Intracytoplasmic tagging of cells with ferumoxides and transfection agent for cellular magnetic resonance imaging after cell transplantation: methods and techniques. Transplantation 2003; 76:1123-1130.
26. Josephson L, Tung CH, Moore A, Weissleder R. High-efficiency intracellular magnetic labeling with novel superparamagnetic-Tat peptide conjugates.

Bioconjug Chem 1999; 10:186-191.

27. Walczak P, Kedziorek DA, Gilad AA, Lin S, Bulte JW. Instant MR labeling of stem cells using magnetoelectroporation. Magn Reson Med 2005; 54:769-774.

28. van den Bos EJ, Wagner A, Mahrholdt H, Thompson RB, Morimoto Y, Sutton BS, et al. Improved efficacy of stem cell labeling for magnetic resonance imaging studies by the use of cationic liposomes. Cell Transplant 2003; 12:743-756.

29. Song HT, Choi JS, Huh YM, Kim S, Jun YW, Suh JS, et al. Surface modulation of magnetic nanocrystals in the development of highly efficient magnetic resonance probes for intracellular labeling. J Am Chem Soc 2005; 127:9992-9993.

30. Conner SD, Schmid SL. Regulated portals of entry into the cell. Nature 2003; 422:37-44.

31. Nakase I, Niwa M, Takeuchi T, Sonomura K, Kawabata N, Koike Y, et al. Cellular uptake of arginine-rich peptides: roles for macropinocytosis and actin rearrangement. Mol Ther 2004; 10:1011-1022.

32. Kaplan IM, Wadia JS, Dowdy SF. Cationic TAT peptide transduction domain enters cells by macropinocytosis. J Control Release 2005; 102:247-253.

33. Sorgi FL, Bhattacharya S, Huang L. Protamine sulfate enhances lipid-mediated gene transfer. Gene Ther 1997; 4:961-968.

34. Weber A, Pedrosa I, Kawamoto A, Himes N, Munasinghe J, Asahara T, et al. Magnetic resonance mapping of transplanted endothelial progenitor cells for therapeutic neovascularization in ischemic heart disease. Eur J Cardiothorac Surg 2004; 26:137-143.

35. Himes N, Min JY, Lee R, Brown C, Shea J, Huang X, et al. In vivo MRI of embryonic stem cells in a mouse model of myocardial infarction. Magn Reson Med 2004; 52:1214-1219.

36. Hill JM, Dick AJ, Raman VK, Thompson RB, Yu ZX, Hinds KA, et al. Serial

cardiac magnetic resonance imaging of injected mesenchymal stem cells. Circulation 2003; 108:1009-1014.

37. Dick AJ, Guttman MA, Raman VK, Peters DC, Pessanha BS, Hill JM, et al. Magnetic resonance fluoroscopy allows targeted delivery of mesenchymal stem cells to infarct borders in Swine. Circulation 2003; 108:2899-2904.

38. Kraitchman DL, Heldman AW, Atalar E, Amado LC, Martin BJ, Pittenger MF, et al. In vivo magnetic resonance imaging of mesenchymal stem cells in myocardial infarction. Circulation 2003; 107:2290-2293.

39. Garot J, Unterseeh T, Teiger E, Champagne S, Chazaud B, Gherardi R, et al. Magnetic resonance imaging of targeted catheter-based implantation of myogenic precursor cells into infarcted left ventricular myocardium. J Am Coll Cardiol 2003; 41:1841-1846.

40. He G, Hao Z, Wei H, Yi W, Zhang X, Yue T, et al. In vivo imaging of bone marrow mesenchymal stem cells transplanted into myocardium using magnetic resonance imaging: A novel method to trace the transplanted cells. Int J Cardiol 2006.

41. Rickers C, Gallegos R, Seethamraju RT, Wang X, Swingen C, Jayaswal A, et al. Applications of magnetic resonance imaging for cardiac stem cell therapy. J Interv Cardiol 2004; 17:37-46.

42. Selye H, Bajusz E, Grasso S, Mendell P. Simple techniques for the surgical occlusion of coronary vessels in the rat. Angiology 1960; 11:398-407.

43. Spadaro J, Fishbein MC, Hare C, Pfeffer MA, Maroko PR. Characterization of myocardial infarcts in the rat. Arch Pathol Lab Med 1980; 104:179-183.

44. Jensen JA, Kosek JC, Hunt TK, Goodson WH, 3rd, Miller DC. Cardiac cryolesions as an experimental model of myocardial wound healing. Ann Surg 1987; 206:798-803.

45. Wang YX, Hussain SM, Krestin GP. Superparamagnetic iron oxide contrast agents: physicochemical characteristics and applications in MR imaging. Eur Radiol 2001; 11:2319-2331.

46. Kraitchman DL, Tatsumi M, Gilson WD, Ishimori T, Kedziorek D, Walczak P, et al. Dynamic imaging of allogeneic mesenchymal stem cells trafficking to myocardial infarction. Circulation 2005; 112:1451-1461.
47. Janssens S, Dubois C, Bogaert J, Theunissen K, Deroose C, Desmet W, et al. Autologous bone marrow-derived stem-cell transfer in patients with ST-segment elevation myocardial infarction: double-blind, randomised controlled trial. Lancet 2006; 367:113-121.
48. Hendrikx M, Hensen K, Clijsters C, Jongen H, Koninckx R, Bijnens E, et al. Recovery of regional but not global contractile function by the direct intramyocardial autologous bone marrow transplantation: results from a randomized controlled clinical trial. Circulation 2006; 114:I101-107.
49. Amado LC, Schuleri KH, Saliaris AP, Boyle AJ, Helm R, Oskouei B, et al. Multimodality noninvasive imaging demonstrates in vivo cardiac regeneration after mesenchymal stem cell therapy. J Am Coll Cardiol 2006; 48:2116-2124.
50. Jiang W, Ma A, Wang T, Han K, Liu Y, Zhang Y, et al. Homing and differentiation of mesenchymal stem cells delivered intravenously to ischemic myocardium in vivo: a time-series study. Pflugers Arch 2006; 453:43-52.
51. Jiang W, Ma A, Wang T, Han K, Liu Y, Zhang Y, et al. Intravenous transplantation of mesenchymal stem cells improves cardiac performance after acute myocardial ischemia in female rats. Transpl Int 2006; 19:570-580.
52. Tang J, Xie Q, Pan G, Wang J, Wang M. Mesenchymal stem cells participate in angiogenesis and improve heart function in rat model of myocardial ischemia with reperfusion. Eur J Cardiothorac Surg 2006; 30:353-361.
53. Zhang S, Zhang P, Guo J, Jia Z, Ma K, Liu Y, et al. Enhanced cytoprotection and angiogenesis by bone marrow cell transplantation may contribute to improved ischemic myocardial function. Eur J Cardiothorac Surg 2004; 25:188-195.

ABSTRACT (IN KOREAN)

자기공명영상을 이용한 심근경색모델에 주입된 간엽줄기세포의 생체내 영상화

<지도교수 최규옥>

연세대학교 대학원 의학과

김영진

연구목적: 이 연구의 목적은 자기적으로 표지된 간엽줄기세포를 백서의 심근경색모델에 주입하였을 때 생체내에서 자기공명영상(MRI)을 이용하여 주입된 세포를 영상화하고 동시에 심장기능을 측정할 수 있는지 알아보기 위해서이다.

연구대상 및 방법: 수컷 백서(SD rat)의 심장에 냉동손상을 주어 심근경색을 유발하였다. 인간간엽줄기세포를 초자기적 산화철입자인 Feridex로 표지하고 냉동손상 후 3주가 지난 경색심근에 주입하였고 대조군에는 세포가 포함되지 않은 배지를 주입하였다. 1.5 테슬라 MRI기계와 47mm 의 미세코일을 이용하여 3개월간 백서가 살아있는 상태에서 영상을 얻었다. 세포의 생체 내 추적을 위해서는 심전도 동기화를 이용한 경사에코열을 이용하여 영상을 얻었고, 심장 기능을 측정하기 위해 cine 영상에서 좌심실 구출율을 계산하였다.

연구결과: Feridex로 표지된 간엽줄기세포는 생체 내 MRI에서 주입 후 10주까지 신호감소영역으로 관찰되었다. 장기추적 MRI에서 좌심실

구출율은 대조군 (34.0±2.2%)에 비해 세포주입군 (54.5±4.5%)에서 유의하게 증가된 소견을 보였다.

결론: MRI는 주입된 세포를 생체 내에서 추적할 수 있으며 동시에 심장의 기능을 측정할 수 있어 심근경색의 세포치료의 치료효과를 판정하는데 도움을 줄 수 있다.

핵심되는 말: 자기공명영상, 산화철, 심근경색, 간엽줄기세포, 백서